ZESZYTY NAUKOWE POLITECHNIKI ŁÓDZKIEJ
Nr 1078 ELEKTRYKA z. 121 2010

RADOSŁAW WAJMAN, JACEK NOWAKOWSKI
DARIUS STYRA
Faculty of Electrical, Electronic, Computer and Control Engineering
Technical University of Lodz

IMPROVEMENT OF ELECTRICAL CAPACITANCE TOMOGRAPHY HARDWARE

Recenzent: **doc. dr hab. inż. Roman Szabatin**

Maszynopis dostarczono: 1. 10. 2010

Electrical Capacitance Tomography (ECT) is used to obtain the permittivity distribution of material, measuring capacitances between electrodes, placed around material. ECT is fast, non-invasive and low cost imaging system. A particular difficulty with capacitance measurement of ECT hardware is to measure small capacitance changes between electrodes of sensors having large stray and standing capacitances. The paper consists of two main parts: Improvement of AC – based ECT new a compact ECT hardware. Improved AC-based ECT hardware is more stable, flexible, effective and suitable for electrical conductance tomography; new concepts for hardware design and measurement algorithm are presented and proved by simulation. A new generation, completely different from classical ECT hardware is presented as a Compact ECT. The main advantages of compact ECT hardware are compact size, low power consumption and low price; these advantages achieved using new method of stray capacitance compensation.

1. INTRODUCTION

Electrical Capacitance Tomography (ECT) is a method to obtain permittivity distribution of mixture by measuring capacitances between electrodes placed around the sensing area. ECT systems (Fig. 1) are used for multiphase flow detection in the oil industry [1], chemistry [2], agriculture [3] and in research.

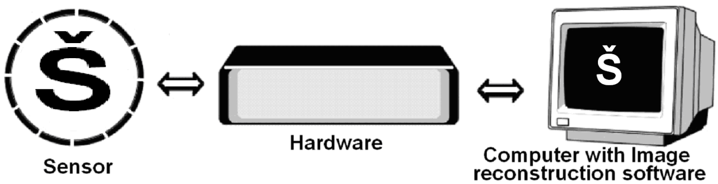

Fig. 1. Electrical capacitance tomography system

In the last two decades AC-based ECT techniques have made a big progress in terms of software for image reconstruction [4, 5] and hardware, especially digital electronics parts [6-7]. On the other hand analog electronics has known only few improvements and the main principle remains the same, i.e. the use of charge amplifier [8] or so called auto-balancing bridge [9].

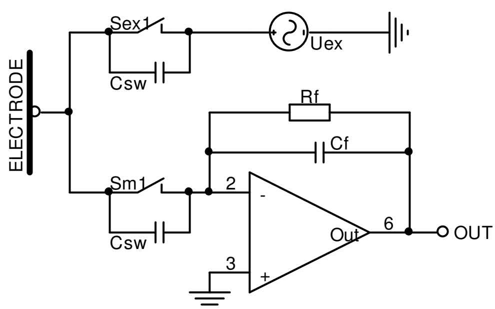

Fig. 2. Electronic circuit for one electrode in ECT hardware

Use of charge amplifier (Fig. 2) makes the tomograph stray capacitance immune by allowing voltage excitation and current measurement principle for capacitance measurement [10]. One of the most significant changes in analog part of electronics was the use of three switches to connect excitation voltage to excitation electrode [11]. This change has the main benefit of increasing capacitance measurement range to lower values by eliminating the influence from capacitance of the switches in OFF mode (C_{sw}) which acts in parallel to the measurement capacitances. Meanwhile, the noise created by non-linear capacitance of the switch is also removed.

With the design described above, the input measurement circuit is working properly, even if it encounters some limitations. The first problem concerns the measurement of capacitances which are much smaller than C_{sw}. It has been found that the input circuit has a too large input signal and the output voltage goes into saturation when the electrodes are switched into excitation mode because of the C_{sw} coupling. The capacitance C_{sw} depends on the chosen switch and varies from one to hundreds of pF while capacitances between electrodes in ECT sensors can be less than 10 fF. Non linear distortions appear because of signal saturation, temperature increases [12] and hardware becomes instable.

Another problem concerns the sensitivity of the input circuit which usually lacks of flexibility. Indeed, the sensitivity of the input circuit depends on the feedback of the charge amplifier. Impedance of tenths of kilo Ohms is used as a feedback to make the input circuit sensitive enough. This generates an impedance of feedback (parallel junction of R_f and C_f in Fig. 2) which is larger than the impedance of switch in OFF mode because of a too large C_{sw}. Therefore, the switch cannot be used normally. Hardware is not flexible and cannot be switched to resistance or conductance mode where the sensitivity of the input circuit should be decreased up to a thousands times.

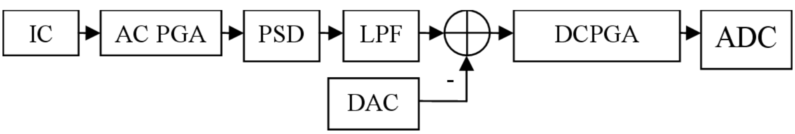

Fig. 3. Principle of measurement signal acquisition

The last limitation concerns the standard protocol to calibrate ECT hardware in order to normalize the capacitance measurement. The first calibration is made for the sensing area being empty in order to eliminate the standing capacitances by setting offset values in DAC (Fig. 3). The second calibration point is made for the sensing area filled with high permittivity mixture and DC gains (in Fig. 3) are calibrated by setting them as high as possible. Non flexible algorithm of AC gains is used [11].

Based on above limitations, an improved AC-based ECT hardware is described in this paper. The hardware developed by Yongbo He et al. [7] was modified and corresponding improvement are described in the three following sections. The first section describes the method to improve switch combination for electrode connection to charge amplifier in order to obtain a more stable hardware. The following section presents the new feedback switching circuit that allows changing sensitivity of input circuit. The last section, before the conclusion, is devoted to the methodology used for the obtaining of an additional calibration step for AC gains in order to improve the flexibility of the hardware in order to accommodate any kind of 2D or 3D ECT sensor layouts.

Above mentioned virtual ground circuit is suitable for “voltage excitation – current measurement” systems, with the excitation usually being sine [11], square [13] or triangle voltage signal [14]. In general, the classical ECT hardware is designed using 19” Euro case and PCBs contain a lot of components which makes the price relatively expensive and power consumption relatively high. Kjærsgaard-Rasmussen and Yang [15] have designed a charge/discharge unit that can hold in a smaller case in order to provide a more portable system. However, it is not easy to use ECT systems, even for the latter compact one, for on-site installation with very limited access and restrictive access to power supply. In that context, a new generation of ECT hardware, based on stray capacitance compensation, is presented. The methodology that is used for the capacitance measurement makes the system completely different from a classical ECT hardware concept. The capacitance discharge time measurement will be used for capacitance measurement. The main advantages of the new system are compact size, low power consumption and low price. The paper is structured as follows. Section 2 presents the general theory of stray capacitance compensation for non-stray immune system. Experimental results to validate the approach are presented in section 3. The new ECT system hardware is presented in section 4 before final conclusions and perspectives of work are mentioned.

The paper consists of two main parts. Improvement of AC – based ECT system described in first part and total new compact ECT hardware with new stray capacitance compensation is described in second part.

2. IMPROVEMENT OF AC-BASED ECT HARDWARE

This section describes improvement of AC-based ECT system in the three following sections. The 2.1 section describes the method to improve switch combination for electrode connection to charge amplifier in order to obtain a more stable hardware. The following section 2.2 presents the new feedback switching circuit that allows changing sensitivity of input circuit. The last section 2.3 is devoted to the methodology used for the obtaining of an additional calibration step for AC gains in order to improve the flexibility of the hardware in order to accommodate any kind of 2D or 3D ECT sensor layouts.

This part of paper is based on paper “Improvement of AC-based Electrical Capacitance Tomography Hardware” [16].

2.1. Electronics connection to sensor electrodes

Nowadays, ECT system can handle from 6 to 32 electrodes. Each electrode operates either in excitation or in measurement mode. The mode is changed by connecting the electrode to excitation or measurement circuit using switches. Switch in OFF mode has capacitance C_{sw}. Electronics with switch combination shown in Fig. 2 is suitable only for ECT sensors with interelectrode capacitance much higher than C_{sw}.

Simulation results have shown that using of one switch S_{m1} for electrode connection to measurement circuit is not enough in some cases. Problem appears when the hardware is used for ECT sensor having capacitance between electrodes much smaller than C_{sw}. In that case the sensitivity of the input circuit should be as high as possible by setting feedback impedance (see parallel combination of C_f and R_f in Fig. 2) as high as possible. However, the increase of feedback impedance is limited not only by the smallest inter-electrode impedance but also by the impedance of S_{m1} in OFF mode. The input current in the charge amplifier resulting from the capacitance C_{sw} of S_{m1} may be too large when the impedance of measurement switch in OFF mode is smaller than the feedback impedance while electrode is working in excitation mode. Consequently, the output voltage presents saturation, harmonic distortions and additional harmonics with high frequency forms. This has direct impact on the system instability and serious damage of the ECT hardware can occur because of the sudden rise of components temperature.

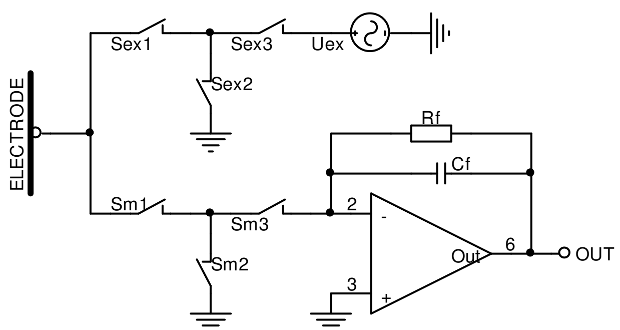

Fig. 4. Input circuit with additional switches S_{m2} and S_{m3} for charge amplifier connection

The new circuit shown in Fig. 4 works as follows. Switches S_{m1} and S_{m3} are in OFF position and switch S_{s2} is in ON position while electrode is set to excitation mode. In the case when electrode is working in measurement mode, the above switches are set to the opposite mode. The decrease of the output voltage in comparison to the standard circuit shown in Fig. 2 is presented in Fig. 5. This comparison has been performed using PSpice simulation.

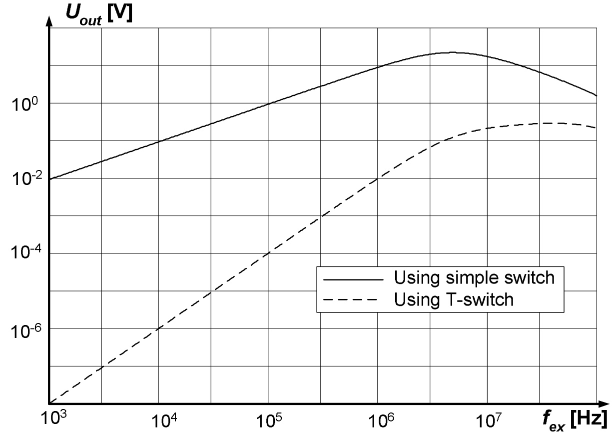

Fig. 5. Frequency dependence of t output voltage U_{out} while input circuit is in excitation mode

One can see from the simulation results that the additional switches S_{m2} and S_{m3} (T-switch) allow decreasing significantly the output voltage by minimizing the parasite current flow to input of the charge amplifier. Output voltage and parasite current were minimized 1820 times at the excitation frequency f_{ex} of 500 kHz.

2.2. Flexible sensitivity of input circuit

AC-based ECT hardware has input circuit based on charge amplifier (Fig. 2) and sensitivity of input circuit is dependent on its feedback [17]. In the case where it is desired that the tomograph works in other modes than for capacitance measurement, ie. to allow resistance or conductance measurement to be done, there is the need to significantly decrease the sensitivity of the input circuit.

One standard way to achieve such requirement is to use additional amplifier with programmable gain [7]. Another way is to use switching feedback as it is shown in Fig. 6. However, using simple switching feedback can have some drawbacks.

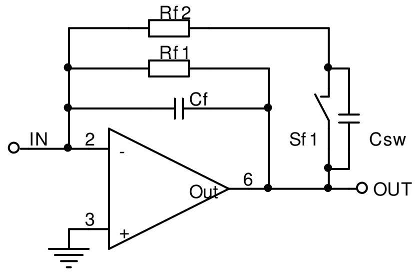

Fig. 6. Charge amplifier with switchable feedback

The PSpice simulation of the switchable feedback circuit shown in Fig. 6 has shown that the sensitivity can be changed to high only for low frequencies. However, standard AC-based ECT hardware uses high frequencies up to 10 MHz [18] and simple feedback switching is therefore not suitable because of the parasite effect from the C_{sw} coupling. Indeed, switch in OFF position has too low isolation and signal passes through the C_{sw} of S_{f1} which inevitably decreases the sensitivity.

One solution that has been already proposed is to use additional switches [19] in order to annihilate the coupling effect from the C_{sw}. This is illustrated in Fig. 7 with the use of switches S_{f2} and S_{f3}.

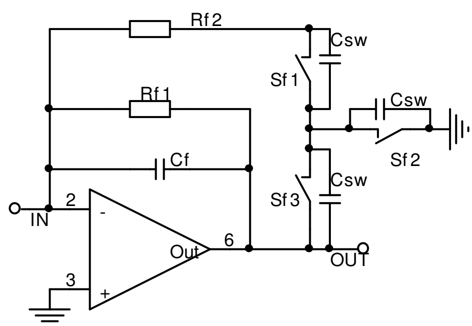

Fig. 7. Switchable feedback for high frequency applications

The comparison between the input circuits in high sensitivity mode shown in Fig. 6 and Fig. 7 was again carried out using PSpice simulation presented in Fig. 8. The corresponding Figure also presents the case with the input circuit having only one feedback resistance R_{f1}.

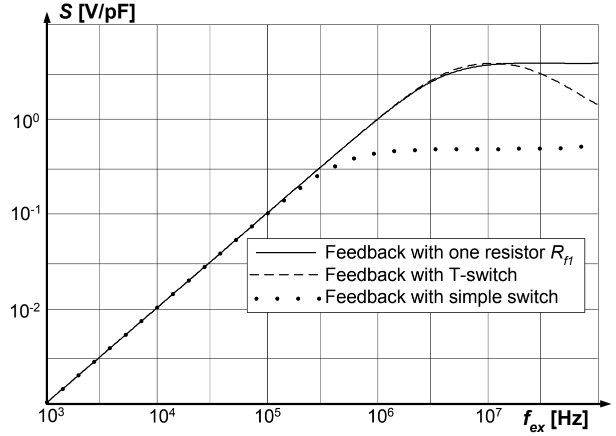

Fig. 8. Frequency dependence of charge amplifier sensitivity S, using different feedback switching circuits: R_{f1}: 33 kΩ, R_{f2}= 51 Ω, C_f= 1.2 pF, R_{sw}= 35 Ω, C_{sw}= 9 pF, C_x= 1 pF

The simulation results given in Fig. 8 has shown that the simple feedback switching circuit presented in Fig. 6 allows switching only up to 100 kHz while the new circuit presented in Fig. 7 can be used to switch feedback up to 14 MHz. The suggested feedback switching made hardware able to change sensitivity of input circuit in all the frequencies used in ECT.

2.3. Algorithm for flexible calibration of hardware

Standard calibration algorithm is optimized only for special sensor or group of sensors [11].

Hardware calibration was improved by adding the AC gains calibration step which's block diagram is shown in Fig. 9a. Calibration of AC gains was made before Offset and DC gains calibration and with the same material like for DC gains calibration inside the sensor.

Before measuring signals DC gains were set to 1 and the offsets for standing capacitances were set to 0 as it is presented in the block diagram in Fig. 9b.

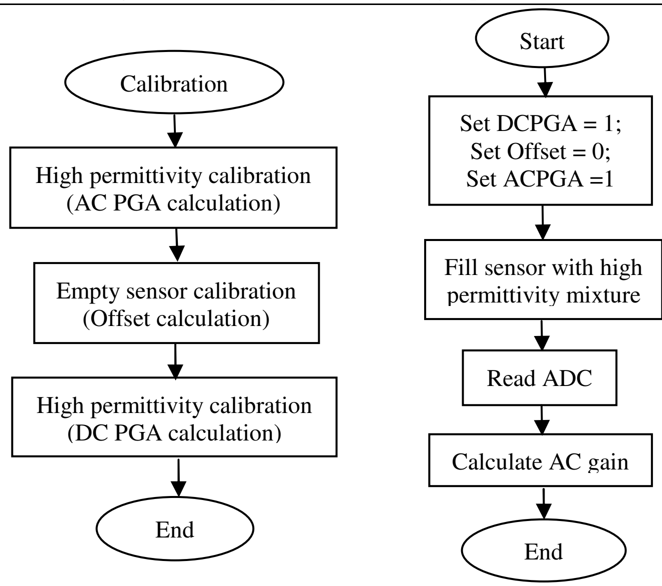

Fig. 9. Calibration algorithms: a – three steps calibration; b – AC gains calibration

AC gains should be set not larger than the division of maximum ADC value by the measured ADC value as it is shown in the equation below.

$$ACPGA \leq K \frac{ADC_{\max}}{ADC_{value}}, \quad (1)$$

here ADC_{max} and ADC_{value} are the – maximal and measured ADC values, respectively; *ACPGA* is the AC programmable gain, K is a safety coefficient.

It is suggested to use safety coefficient $K \approx 0{,}7$ for AC gains. It is difficult to fill sensor in some cases [20] so this coefficient should be used to protect hardware against signal saturation.

Calibration of AC gains by adding additional calibration step allowed compensation of wider range of standing capacitances, allowed to set sensitivity more accurate, made hardware flexible and suitable for any kind of 2D or 3D ECT sensors.

3. COMPACT ECT HARDWARE WITH STRAY CAPACITANCE COMPENSATION

This part describes total new ECT hardware with new stray capacitance compensation method. The section is three following sections. The section 3.1. describes the theory of stray capacitance compensation for non stray immune systems. The following section 3.2. presents the experimental results obtained with new stray capacitance compensation method. The last section 3.3. is devoted to prototype of compact size and low power ECT hardware stray capacitance compensation method.

This part of paper is based on paper "Stray Capacitance Compensation for Non – Stray Immune ECT Systems" which is published in 6th World Congress on Industrial Process Tomography.

3.1. Theory of stray capacitance compensation for non-stray immune systems

ECT sensor is equivalent to multi-electrode system. In that context, the capacitance measurement between two electrodes is influenced by counterparts. Let assume that we have a sensor equipped with 4 electrodes and electrode 5 is ground as schematized in Fig. 10.

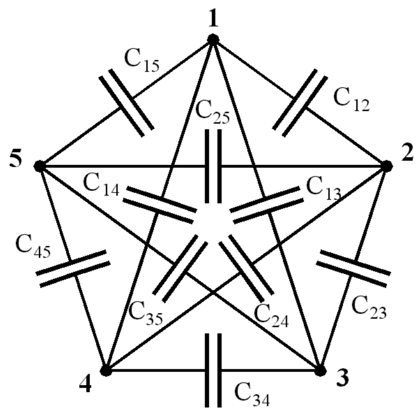

Fig. 10. Multi-electrode capacitance system

The measured capacitance between first and second electrodes $C_{m.12}$ expressed as:

$$C_{m.12} = C_{12} + C_{p.12} \quad (2)$$

here C_{12} is the real capacitance between both electrodes and $C_{p.12}$ is a parasitic capacitance generated by the other electrodes.

3.1.1. Equation solving method

The first method to calculate the real capacitance C_{12} (and the other capacitances) is to express analytically the parasitic capacitance with the other capacitances and solve the set of equations. In the case of a sensor with 5 electrodes, 10 independent measurements are necessary to rebuild the image ($N(N$-1)/2 with N=5 in the present case) which, therefore corresponds to a set of 10 equations with the same number of unknowns. One of these 10 equations corresponding to $C_{m.12}$ is presented below:

$$C_{m.12}=C_{12}+\frac{C_{13}C_{23}}{C_{AA}}+\frac{\left(C_{24}+\frac{C_{23}C_{34}}{C_{AA}}\right)\left(C_{14}+\frac{C_{13}C_{34}}{C_{AA}}\right)}{\frac{C_{23}C_{34}+C_{13}C_{34}+C_{34}C_{35}}{C_{AA}}+C_{14}+C_{45}+C_{24}}+$$

$$+\frac{\left(C_{25}+\frac{C_{23}C_{35}}{C_{AA}}+\frac{\left(C_{24}+\frac{C_{23}C_{34}}{C_{AA}}\right)\left(C_{45}+\frac{C_{34}C_{35}}{C_{AA}}\right)}{\frac{C_{23}C_{34}+C_{13}C_{34}+C_{34}C_{35}}{C_{AA}}+C_{14}+C_{45}+C_{24}}\right)\left(C_{15}+\frac{C_{13}C_{35}}{C_{AA}}+\frac{\left(C_{14}+\frac{C_{13}C_{34}}{C_{AA}}\right)\left(C_{45}+\frac{C_{34}C_{35}}{C_{AA}}\right)}{\frac{C_{23}C_{34}+C_{13}C_{34}+C_{34}C_{35}}{C_{AA}}+C_{14}+C_{45}+C_{24}}\right)}{C_{25}+C_{15}+\frac{C_{23}C_{35}+C_{13}C_{35}}{C_{AA}}+\frac{\left(\frac{C_{23}C_{34}+C_{13}C_{34}}{C_{AA}}+C_{14}+C_{24}\right)\left(C_{45}+\frac{C_{34}C_{35}}{C_{AA}}\right)}{\frac{C_{23}C_{34}+C_{13}C_{34}+C_{34}C_{35}}{C_{AA}}+C_{14}+C_{45}+C_{24}}}$$

(3)

here $C_{AA}=C_{13}+C_{23}+C_{34}+C_{35}$.

The analytical solution for such system of 10 equations is difficult to obtain, but the solution can be solved using minimal error method.

3.1.2. Neglecting method

Some assumptions can be done to simplify the expression of $C_{m.ij}$. Indeed, capacitances with smallest influence can be neglected. For instance, in the case of C_{12} the smallest influence is generated by capacitances C_{34}, C_{35} and C_{45}. These capacitances can be neglected by setting them to zero in equation (3) results in the following simplification:

$$C_{m.12}=C_{12}+\frac{C_{13}\cdot C_{23}}{C_{13}+C_{23}}+\frac{C_{24}\cdot C_{14}}{C_{24}+C_{14}}+\frac{C_{25}\cdot C_{15}}{C_{25}+C_{15}} \quad (4)$$

The set of equations based on the above formula is simpler to solve, but the range of error is larger. Moreover, the solving becomes more and more complicated as the number of electrodes increase (e.g. ECT system with 32 electrodes requires 496 equations to be solved). Therefore there is a need of simpler capacitance measurement method for multi-electrode systems. This is what is presented below with the so-called short-circuiting method.

3.1.3. Short-circuiting method

In this second method, it is assumed that each electrode can be connected to the other electrodes during capacitance measurement and each electrode can be short-circuited independently or simultaneously. For each capacitance $C_{i,j}$ between electrodes i and j, 3 measurements needs to be performed for this method:

1. Capacitance between electrode i and all other short-circuited electrodes:

$$C_{m.i} = \sum_{(k \neq i)} C_{i,k} \quad (5)$$

2. Capacitance between electrode j and all other short-circuited electrodes:

$$C_{m.j} = \sum_{(k \neq j)} C_{j,k} \quad (6)$$

3. Capacitance between connected electrodes j with i and all other short-circuited electrodes:

$$C_{m.i,j} = \sum_{(k \neq i,j)} C_{i,k} + \sum_{(k \neq i,j)} C_{j,k} \quad (7)$$

The real capacitance $C_{i,j}$ is simply expressed as:

$$C_{i,j} = \frac{C_{m.i} + C_{m.j} - C_{m.i,j}}{2} \quad (8)$$

In the case of the real hardware, the capacitance measurement unit is connected to multi-electrode ECT sensor using electronic switches and wires like coaxial cable. Each electrode has capacitance to the shield also. All these components or connection influence the capacitance measurement between each pair of electrodes since they present or generate stray capacitance. Indeed, switches have an influence on the capacitance measurement since switch in OFF mode has capacitance C_{sw} and switch in ON mode has resistance R_{sw}. However, these influences can be eliminated using the short-circuit method as presented below in the case of a sensor with 4 electrodes. The corresponding circuit diagram is presented in Fig. 11 with the different stray capacitances C_{sw} , C_w and C_{sc} of the switches and wires and shield, respectively.

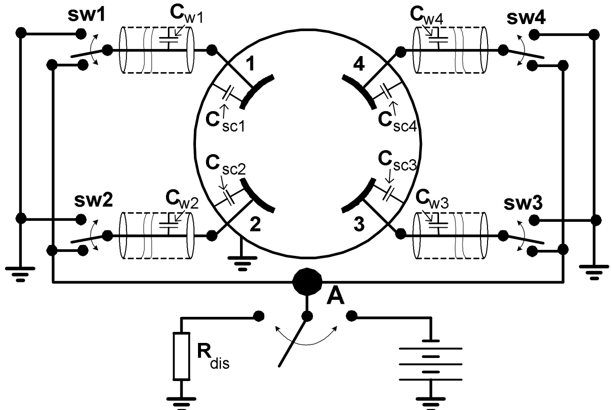

Fig. 11. Circuit diagram for 4 electrode ECT system with capacitances of wires (C_w), switches (C_{sw}) and screen (C_{sc})

The switch A is used for capacitance measurement: switching to DC voltage source for charging and switching to discharge resistor R_{dis} for discharging and discharge time measurement.

In the case of the real capacitance C_{12}, the new set of measurements which takes into account the stray capacitances can be expressed using equations (5) to (7):

1. Capacitance between electrode 1 and all the other short-circuited electrodes:

$$C_{m.1} = C_{12} + C_{13} + C_{14} + C_{w1} + C_{sw2} + C_{sw3} + C_{sw4} + C_{sc1} \quad (9)$$

2. Capacitance between electrode 2 and all the other short-circuited electrodes:

$$C_{m.2} = C_{12} + C_{23} + C_{24} + C_{w2} + C_{sw1} + C_{sw3} + C_{sw4} + C_{sc2} \quad (10)$$

3. Capacitance between connected electrodes 1 with 2 and all other short-circuited electrodes:

$$C_{m.12} = C_{13} + C_{14} + C_{23} + C_{24} + C_{w1} + C_{w2} + C_{sw3} + C_{sw4} + C_{sc1} + C_{sc2} \quad (11)$$

The calculation of real capacitance C_{12} can therefore be expressed as follows using (8):

$$C_{12} = \frac{2C_{12} + C_{sw1} + C_{sw2} + C_{sw3} + C_{sw4}}{2} \quad (12)$$

As it can be seen from equation (12), influences of C_w and C_{sc} are eliminated and only capacitances of all the switches in OFF mode have influence on the real capacitance measurement, resulting in error. The error is the same in all the calculations of $C_{i,j}$ and equal to sum of all the switch capacitances in OFF mode $C_{\Sigma sw}$. In order to compensate this error, and therefore to have a correct expression of equation (12), equation (8) has to be modified as follows:

$$C_{i,j} = \frac{C_{m.i} + C_{m.j} - C_{m.i,j} - C_{\Sigma sw}}{2} \quad (13)$$

Equation (13) illustrates how the method of short-circuiting for compensation of stray capacitances is easy to apply and is independent on the number of electrodes. The capacitance $C_{\Sigma sw}$ is measured when all the electrodes are switched to the ground.

3.1.4. Measurement speed of short-circuiting method

As it has been stated in previous section, the short-circuiting method for the stay compensation is normally independent on the number of electrodes. This is actually an assumption that can be verified by estimating the measurement speed and comparing it with classical stray immune capacitance measurement method. Image reconstruction in ECT is done by using all the independent capacitances between all the electrodes.

Number of single measurements for getting all the independent capacitances using electrode short circuit method is bigger than using stray immune system. There is need to measure all the capacitances $C_{m.i}$, all the capacitances $C_{m.i,j}$ and sum of all the switch capacitances $C_{\Sigma sw}$. Total sum of single measurements number M is dependent on number of electrodes N

$$M = N + \frac{N(N-1)}{2} + 1 \quad (14)$$

The difference ration D of single measurements number in stray immune and in non-stray immune systems needed to get all the independent capacitances is dependent on the electrode number N (Table 1).

Table 1. Difference in single measurement numbers using stray immune and non-stray immune methods

	Single measurement number					
Electrode number N	6	8	10	12	16	32
Stray immune M	15	28	45	66	120	496
Stray compensated M	22	37	56	79	137	529
Difference D	1.467	1.321	1.244	1.197	1.142	1.067

The calculation result given in table.1 has shown that difference ratio *D* between single measurements numbers is smaller when electrode number is greater. The measurement speed can be increased by using rapid measurement methods, i.e. a capacitance discharge time measurement. In the following section, experimental comparison of different methods is presented.

3.2. Experimental results

3.2.1. Comparison of methods

This sub-section focuses on the comparison of the above methods to compensate stray capacitances. The experimental comparison was done on a sensor equipped with 5 electrodes. Measurements between electrodes #1 and #2 and electrodes #4 and #5 were considered and the calculation of the real capacitances and measurements were performed based on the consideration described in the previous section, i.e. *equation solving method*, method with neglected some stray capacitances (called hereafter *neglecting method*), the *short-circuiting method*, the *direct method* (without stray capacitance compensation) and method that only consider two electrodes without surrounding ones (*isolated method*). The latter case was obtained by separating the multi-electrode system into two sets of 2 electrodes after measurements for the other methods were done, as it is schematized in Fig. 12.

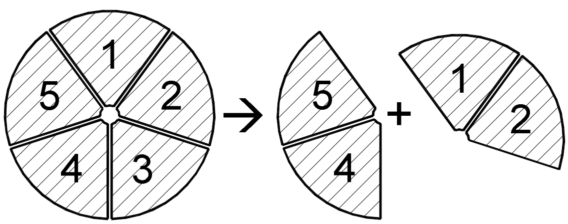

Fig. 12. Conversion from multi-electrode sensor to 2 sets of 2 electrodes

The two capacitances for the *isolated method* were measured with the assumption that these capacitances are real since there is normally no interaction with other electrodes or capacitance influence from any surrounding device. The results for all measurement methods are presented in Table 2. Calculation of errors made assuming that the real capacitances are the measurement results of isolated method.

Table 2. Comparison of measurement methods

Method	C_{12}, pF	C_{45}, pF	Error		Relative error	
			C_{12}, pF	C_{45}, pF	C_{12}, %	C_{45}, %
1. Equation solving	2.259	2.046	-0.015	-0.024	0.66%	1.16%
2. Neglecting	2.079	1.920	-0.195	-0.15	8.58%	7.25%
3. Short-circuiting	2.258	2.072	-0.016	0.002	0.70%	0.10%
4. Without compensation	2.563	2.382	0.289	0.312	12.71%	15.1%
5. Isolated	2.274	2.070	0.000	0.000	0.00%	0.00%

One can see from experimental results that the largest error obtained using the neglecting method, and the small error is obtained using the short-circuiting method. The method of direct measurement gives error larger than 15%.

3.2.2. Stray capacitance compensation for ECT sensor

Method of short-circuiting tested on the two different 12 electrode ECT sensors. Agilent E4980A precision RLC meter with Option001 used for capacitance measurement. Capacitances between adjacent electrodes (1 and 2) and opposite electrodes (1 and 7) were measured using stray capacitance immune and stray capacitance compensation methods. Table 3 presents measurement results.

Table 3. Capacitance between electrodes measurement results

Sensor	electrodes	method	C, fF	U*, fF	U*, %	diff*, fF	diff*, %
1*, empty	1 – 2	Stray immune	424.058	0.562	0.133	0.004	0.00
1*, empty	1 – 2	Stray compensated	424.062	0.311	0.073		
1*, empty	1 – 7	Stray immune	4.158	0.169	4.069	-0.057	-1.38
1*, empty	1 – 7	Stray compensated	4.101	0.093	2.268		
2*, full	1 – 2	Stray immune	2249.514	0.566	0.025	0.353	0.02
2*, full	1 – 2	Stray compensated	2249.867	0.313	0.014		
2*, full	1 – 7	Stray immune	30.821	0.433	1.016	0.494	1.59
2*, full	1 – 7	Stray compensated	31.315	0.238	0.760		

U* - uncertainty type A, p=95%; diff* - difference between measurement results; 1* - sensor with 160 mm diameter, electrode length 160mm and 25 mm electrode width; 2* - sensor with 45 mm diameter, electrode length 100mm and 9.5 mm electrode width.

One can see from experimental results that the measurement results using both methods are almost the same for the capacitance between adjacent electrodes and not exceeding 1.6% for capacitance between opposite electrodes.

3.3. Prototype of compact size and low power ECT hardware

The block diagram of the hardware prototype is presented in Fig. 13.

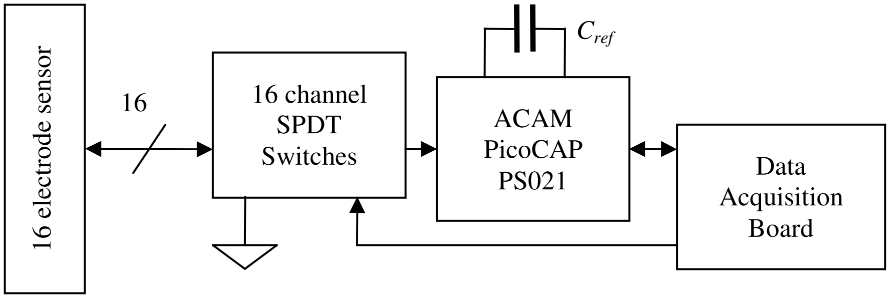

Fig. 13. Block diagram of compact size low power ECT hardware

Microchip PS021 is used for capacitance measurement. This microchip is based on capacitance discharge time measurement and allows measurement rate up to 50 kHz, resolution up to 6 aF, wide range of capacitances (0fF – 10nF) and has extremely low current consumptions (down to 10μA), but this microchip is not stray capacitance immune. Above described stray capacitance compensation method and capacitance measurement microchip PS021 allows to design new, compact size, stray immune and powered by battery ECT hardware.

Each electrode should be connected either to ground or to measurement circuit. It is enough only one SPDT switch per electrode while using classical stray immune system at least 4 switches are needed 11. The one switch per electrode allows switch mounting directly on electrode and minimizes the biggest stray capacitance – capacitance of coaxial cable C_w 21. The design of compact size, low power and low price ECT hardware prototype is shown in Fig. 14.

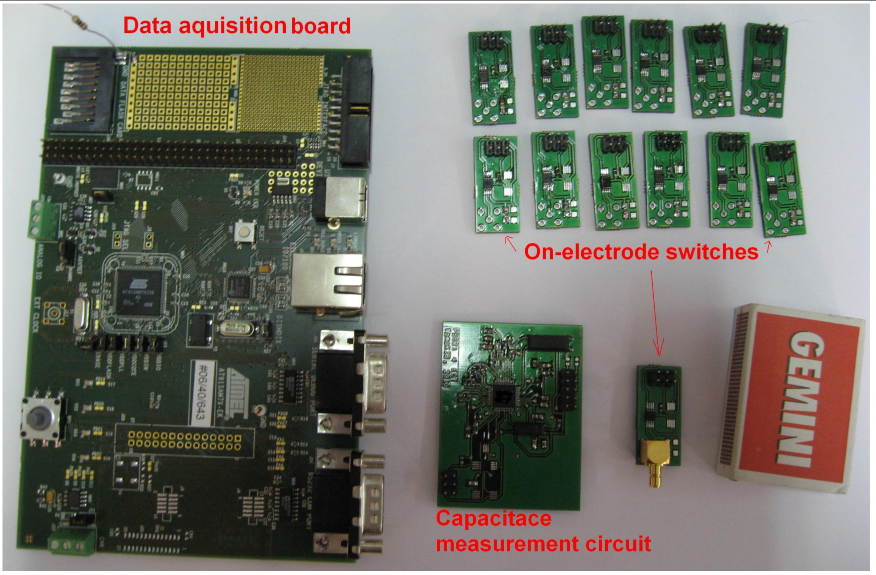

Fig. 14. Prototype of compact size, low power and low price ECT hardware

The prototype of hardware designed for up to 16 electrode sensors and can be easily extended by adding additional switch circuits. Switch circuits and the capacitance measurement circuit are controlled by data acquisition board. Data acquisition board with the high-performance microcontroller (AT91SAM7X) is used for high speed applications and ultra-low-power microcontroller (MSP430) is used for powered by battery data acquisition board.

4. EXPERIMENT AND CONCLUSIONS

Using the described ECT measurement unit and a 8 electrodes sensor some measurements with the mixture of oil and air were performed. In the figure 15 below two images are shown. The images were reconstructed from ECT measurements performed for mixtures containing respectively 20% and 50% of oil. As an image reconstruction algorithm the common Landweber iterational method was chosen. 100 iterations were calculated with the relaxation parameter equal to 0.5. Red color on the images points the regions where the oil appeared during the experiment.

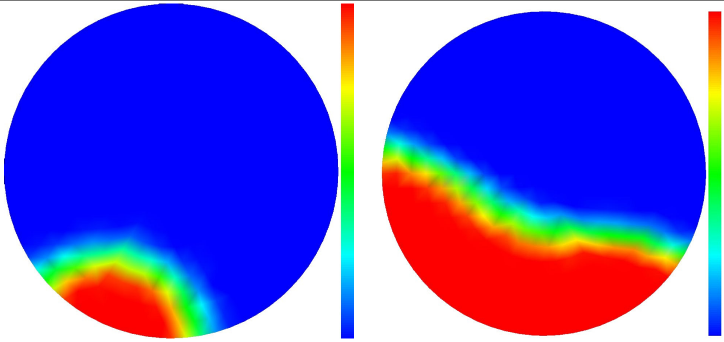

Fig. 15. Reconstructed images of mixture oil and air

The following conclusion can be drawn concerning the improvement of AC-based ECT hardware:

- Additional switches for electrodes connection to measurement circuits prevent hardware from signal saturation, which is accompanied by a significant drop of the hardware temperature and therefore minimization of power dissipation.
- Suggested feedback switching for charge amplifier makes ECT hardware more flexible and suitable for ERT measurements.
- Additional calibration point allows calibration of AC gains to be made which results in a more flexible system that can be more suitable for any kind of 2D or 3D sensors, especially when the distance between electrodes located in different planes need to be compensated.

The following conclusion can be drawn concerning a new concept of ECT hardware based on a new method for stray capacitance compensation. The new method allows using of all known capacitance measurement methods for ECT. Designed compact size, low power and low price ECT hardware can be powered by battery. The system can be used in deep sub sea oil wells near by end of pipes.

ACKNOWLEDGEMENTS

The work is funded by the European Community's Sixth Framework Programme – Marie Curie Transfer of Knowledge Action (DENIDIA, contract No.: MTKD-CT-2006-039546).

REFERENCES

[1] **Ismail I., Gamio J. C., Bukhari S. F. A., Yang W. Q.** Tomography for multi-phase flow measurement in the oil industry // *Flow Meas. Instrum.*, 2005. -16. - P.145-155.

[2] **Tapp H. S., Peyton A. J., Kemsley E. K., Wilson R. H.** Chemical engineering applications of electrical process tomography *// Sensors and Actuators, B: Chemical*, 2003. -92. - P.17-24.

[3] **Grudzien K., Romanowski A., Chaniecki Z., Niedostatkiewicz M., Sankowski D.** Description of the silo flow and bulk solid pulsation detection using ECT *// Flow Meas. Instrum.* Volume 21, Issue 3, September 2010, Pages 198-206

[4] **Yang W. Q., Peng L.** Image reconstruction algorithms for electrical capacitance tomography *// Measurement Science and Technology*, 2003. -14.

[5] **Banasiak R., Soleimani M.** Shape based reconstruction of experimental data in 3D electrical capacitance tomography *// NDT and E International, 43 (3), pp. 241-249*

[6] **Huang S., Green R. G., Plaskowski A., Beck M. S.** A high frequency stray-immune capacitance transducer based on the charge transfer principle *// Instrumentation and Measurement, IEEE Transactions on*, 1988. -37. - P.368-373.

[7] **YongBo H., Radosław W., Robert B., Meng X., Dominik S.,** Design of TCP/IP Based Flexible Three Dimensional Electrical Capacitance Tomography, 2009. -2. - P.1-6.

[8] **Erling A. Hammer** Multi modality tomography systems - State of the art and possible future applications, 2008. - P.1-8.

[9] **Dumbrava V., Svilainis L.** The Automated Complex Impedance Measurement System *// ELECTRONICS AND ELECTRICAL ENGINEERING*. - Kaunas, Technologija, 2007. -2007. Nr. 4(76). - P.59-62.

[10] **Kuroda S.** Simple stray-free capacitance meter by using an operational amplifier. *// IEEE Transactions on Instrumentation and Measurement*, 1983. -IM-32. - P.512-513.

[11] **Yang W. Q., York T. A.** New AC-based capacitance tomography system *// Science, Measurement and Technology, IEE Proceedings* -, 1999. -146. - P.47-53.

[12] **Vamos A.** Design of High Temperature Operational Amplifiers. *// Meres es automatika*, 1981. -29. - P.169-176.

[13] **Brzeski P., Mirkowski J., Olszewski T., Plaskowski A., Smolik W., Szabatin R.** Multichannel capacitance tomograph for dynamic process imaging *// Opto-electronics Review*, 2003. -11. - P.175-180.

[14] **Betiuk J.** Differential measure methods in electrical capacitance tomography *// Proceedings of Electrotechnical Institute*. - Instytut Elektrotechniki, 2008. -238. - P.147-157.

[15] **Kjærsgaard-Rasmussen J., Yang W. Q.** A compact electrical capacitance tomography system *// IST 2008 - IEEE Workshop on Imaging Systems and Techniques Proceedings*, 2008. - P.175-180.

[16] **Styra D., Babout L.** Improvement of AC-based Electrical Capacitance Tomography Hardware *// Elektronika ir Elektrotechnika*, 2010. - P.47-50.

[17] **Sheng-Yu Peng, Qureshi M. S., Hasler P. E., Hall N. A., Degertekin F. L.** High SNR capacitive sensing transducer *// Circuits and Systems, 2006. ISCAS 2006. Proceedings. 2006 IEEE International Symposium on*, 2006. - P.4 pp.-1178.

[18] **Marashdeh Q., Fan L. -., Du B., Warsito W.** Electrical Capacitance Tomography - A Perspective *// Ind Eng Chem Res*, 2008. -47. - P.3708-3719.

[19] **Im D., Kim H. -., Lee K.** A CMOS resistive feedback differential low-noise amplifier with enhanced loop gain for digital TV tuner applications // *IEEE Trans. Microwave Theory Tech.*, 2009. -57. - P.2633-2642.

[20] **Hadi B., Berruti F., Briens C.** New calibration methods for accurate electrical capacitance tomography measurements in particulate-fluid systems // *Industrial and Engineering Chemistry Research*, 2009. -48. - P.274-280.

[21] **Yang W. Q., Stott A. L., Gamio J. C.** Analysis of the effect of stray capacitance on an ac-based capacitance tomography transducer // *Instrumentation and Measurement, IEEE Transactions on*, 2003. -52. - P.1674-1681.

MODYFIKACJA UKŁADU POMIAROWEGO W ELEKTRYXCZNYM TOMOGRAFIE POJEMNOŚCIOWYM

Streszczenie

Elektryczna tomografia pojemnościowa (ECT) jest stosowana w celu pozyskania rozkładu przenikalności elektrycznej badanego materiału umieszczonego pomiędzy elektrodami. Technika ECT jest szybkim, nieinwazyjnym i tanim system diagnostycznym. Prawdziwym wyzwaniem dla konstruktorów systemów ECT jest opracowanie sprzętu elektronicznego do pomiaru bardzo małych zmian pojemności między elektrodami czujnika dodatkowo obarczonych dużymi wartościami pojemności rozproszonych i pasożytniczych. Bieżąca praca rozwiązuje dwa problemy: poprawa obwodów pomiarowych AC systemu ECT o nowy kompaktowy sprzęt przez co pomiar jest bardziej stabilny i dokładny. Nowa koncepcja w zakresie projektowania sprzętu oraz algorytm pomiaru została potwierdzona poprzez symulację. Dodatkowo autorzy przedstawiają nowe rozwiązanie w wersji mobilnej - kompaktowej. Główne zalety kompaktowych tomografów ECT są ich niewielkie rozmiary, niski pobór mocy oraz niska cena.

Politechnika Łódzka
Katedra Informatyki Stosowanej